

## Differential Cross Section for Coherent Photon Scattering from ${}^4\text{He}$ at 180 MeV

E. J. Austin, E. C. Booth, E. K. McIntyre, J. P. Miller, B. L. Roberts, and D. A. Whitehouse  
*Boston University, Boston, Massachusetts 02215*

and

G. Dodson  
*Massachusetts Institute of Technology, Cambridge, Massachusetts 02139*  
(Received 14 May 1986)

We report the measurement of the differential scattering cross section for coherent photon scattering (nuclear Compton scattering) from  ${}^4\text{He}$  at an average energy of 180 MeV. This represents the first direct observation of the coherent process on a complex nucleus above the pion threshold. The results are compared with the prediction of a calculation utilizing the isobar-hole formalism.

PACS numbers: 25.20.Dc, 25.10.+s

For many years, the scattering of low-energy photons has been a useful tool for studying nuclear dynamics. In contrast, at energies above the pion photoproduction threshold (140 MeV), photon scattering will provide information about the intermediate propagation of pions and isobars in the nuclear medium which is complementary to that obtained from pion scattering and pion photoproduction.

Both pion-nucleus scattering and pion photoproduction involve the strong interaction in the ingoing or outgoing states and therefore nuclear-surface interactions dominate.<sup>1</sup> Photon scattering occurs throughout the nucleus, however, and there is no distortion of the incident and outgoing photon. Any deviation of the cross section from that given by a plane-wave impulse approximation is direct evidence of nuclear-medium corrections to the elementary nucleon-photon scattering amplitude. Of particular interest is coherent photon scattering, where the residual nucleus is left in its ground state. The theoretical interpretation is made simpler since the ground-state properties of the target nucleus are usually well known. Also, by use of the optical theorem and dispersion relations the forward elastic-scattering amplitude can be related to independent measurements of the total photoabsorption cross sections.

The coherent-photon-scattering cross sections are very small and the energy resolution in the detection of the scattered photon must be sufficient to exclude inelastic scattering as well as the decay photons from  $\pi^0$  photoproduction. Consequently, elastic-scattering experiments are difficult to carry out above the pion threshold, and existing scattering data from complex nuclei are limited. The proton represents an exception, where a favorable recoil energy and a cross section that depends less strongly on the scattering angle have led to good data<sup>2</sup> in the resonance region by the recoil technique for  $\theta_{\text{lab}} > 50^\circ$  and  $E_\gamma > 240$  MeV.

Hayward and Ziegler<sup>3</sup> recently reported data by detection of the scattered photon directly at  $\theta_{\text{lab}} = 115^\circ$  for  ${}^{12}\text{C}$  and  ${}^{208}\text{Pb}$  for a number of energies between 150 and 400 MeV. Their  ${}^{12}\text{C}$  cross sections agree with an isobar-hole calculation<sup>1</sup> at 200 MeV but are 2 orders of magnitude above the calculation at 325 MeV. However, their 10% energy resolution was not sufficient to distinguish coherent from inelastic scattering. Recent calculations<sup>4</sup> of the incoherent contribution to the  $(\gamma, \gamma)$  cross section for  ${}^{12}\text{C}$  and  ${}^{208}\text{Pb}$  indicates that it can be large at back angles compared to the coherent cross section, especially at energies approaching the  $\Delta$  resonance and higher.

We report the first direct measurement of coherent nuclear photon scattering above the pion threshold. This experiment was performed at the Massachusetts Institute of Technology Bates Linear Accelerator by use of bremsstrahlung with a 10-cm liquid- ${}^4\text{He}$  target. This target was chosen because of the large energy gap between the ground and excited states in  ${}^4\text{He}$ .

The photons were detected with a shielded  $30 \times 30 \times 30\text{-cm}^3$  NaI(Tl) array consisting of nine  $10 \times 10 \times 30\text{-cm}^3$  elements. The detector was surrounded on all sides except the back, by 2.5-cm-thick plastic-scintillator cosmic-ray veto counters. The detector aperture was defined by a  $10 \times 10\text{-cm}^2$  tungsten collimator.

In order to determine the NaI efficiency, it was necessary to understand in detail its energy response function. The measured response to 190-MeV electrons incident on the center of the central detector, which is very similar to its response to photons, is shown in Fig. 1. The agreement with the predicted response based on a Monte Carlo simulation of the electromagnetic shower<sup>5</sup> is quite good. A similar comparison between the predicted and the measured response to an incident bremsstrahlung beam also showed good agreement.

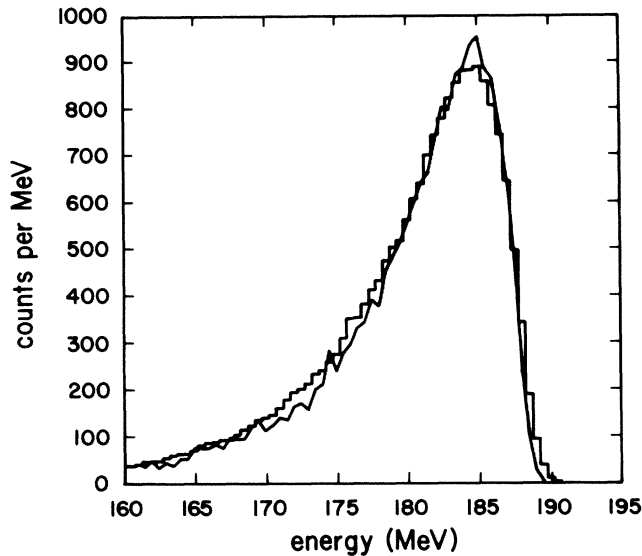


FIG. 1. The response to 190-MeV electrons incident on the center of the detector. The histogram represents the data, and the line, the simulation. The shape is mainly determined by the effects of shower leakage from the crystal.

The electron and bremsstrahlung data were used to establish the energy calibration of the detector. The calibration agreed with that obtained from a 4.6-MeV gamma source to within 2.0%. Gain stability was checked by collection of 4.6-MeV gamma spectra between data runs. In addition, each NaI element was connected by optical fibers to a common calibrated LED light source which was triggered randomly to monitor rate-dependent gain shifts and pulse pileup.

At forward angles, pileup due to low-energy photons from electron Compton scattering of the incident beam in the target limited the maximum bremsstrahlung flux which could be used. For the 30° and 45° data, a 20-cm Be absorber was placed between the target and the detector to suppress low-energy photons and electrons. Veto counters rejected conversion electrons produced in the Be absorber. Wide-angle pairs from the target were swept away by a dipole magnet. The accelerator duty factor was 1%. At  $\theta = 30^\circ$ , the average intensity in the top 20 MeV of the bremsstrahlung spectrum was  $2 \times 10^7/\text{sec}$ .

The scattered-photon spectrum measured at 90° is shown in Fig. 2. At 90°, the maximum scattering-photon energy is 180.8 MeV. Below 153.5 MeV there is a substantial background contribution from  $\pi^0$ -decay photons. For incident photons near the bremsstrahlung end-point energy (190 MeV), the shape of the spectrum is that of the incoming photon beam modified by the response of the detector, by the nuclear-recoil energy loss, and by the energy dependence of the cross section. We simulated the photon-scattering and  $\pi^0$ -decay spectra using the detector

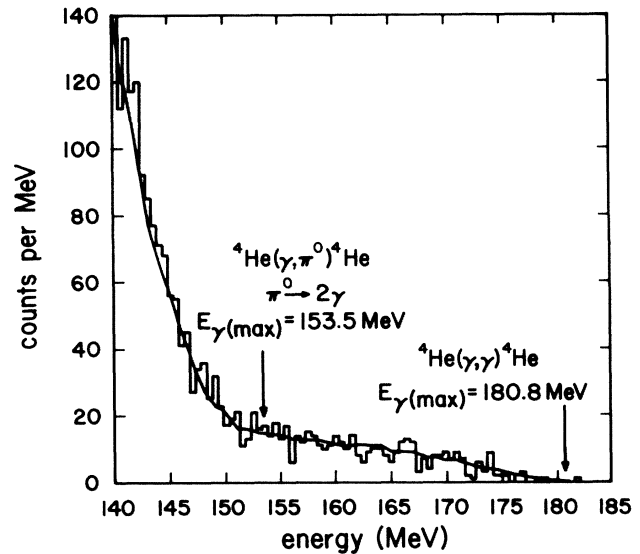


FIG. 2. Histogram, the measured spectrum of photons at 90°. Line, simulation of the shapes of the  $\pi^0$ -decay-photon and the elastic-photon spectra. The amplitudes from the two processes were separately adjusted for a best fit. The maximum photon energy for each process is indicated.

response predicted by an electromagnetic shower code,<sup>5</sup> assuming energy-independent cross sections. As can be seen in Fig. 2, when the amplitudes of the two shapes are adjusted to give the best fit, the positions of the elastic-scattering end point and of the onset of  $\pi^0$  background occur at the correct energies, thereby confirming our energy calibration.

A similar set of fits was attempted for the 30° data (Fig. 3). The end points for the elastic- and decay-photon spectra occur at the proper energies, but there is a dip in the observed spectrum centered approximately 30 MeV below the elastic-scattering end point which leads to a poor fit with the simulated shapes. A better fit (Fig. 3) was obtained by use of dispersion relations as described below to predict the decrease in cross section with energy.

To obtain our final cross sections (Fig. 4), we integrated the data corresponding to incoming photon energies in a range ( $\Delta E$ ) from 20 to 5 MeV below the bremsstrahlung end point. There are no inelastic or  $\pi^0$ -decay photons in this energy range. By not including the top 5 MeV of the incoming photons we reduced considerably the dependence of the cross section on uncertainties in the NaI energy calibration ( $\pm 1.5\%$ ) and uncertainties in the primary beam energy ( $\pm 1\%$ ).

The cross sections were calculated by use of the number of data counts in  $\Delta E$ , the absorption correction in the beryllium absorber and in the target, the number of incident photons in  $\Delta E$ , the solid-angle acceptance, the detector-efficiency correction due to shower leakage ( $\sim 0.55$ ), and the number of target

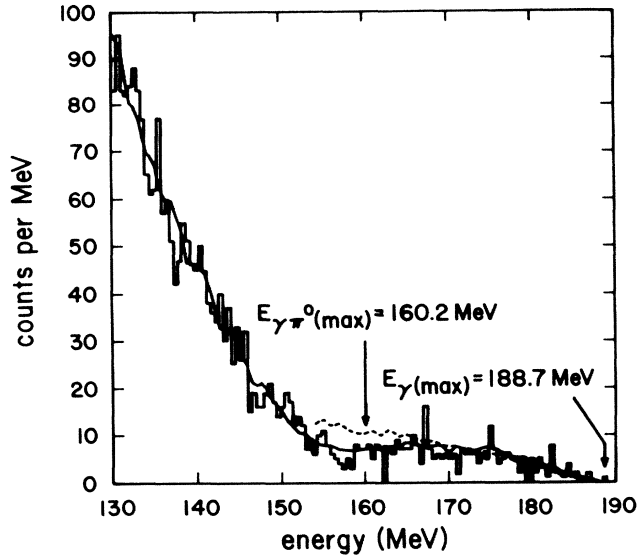


FIG. 3. Histogram, the measured spectrum of photons at  $30^\circ$ . Solid line, as in Fig. 2, except the energy dependence for photon scattering at  $0^\circ$  from dispersion relations has been assumed for the photon scattering. Dashed line, same as solid line except no energy dependence was assumed.

nuclei per unit area. From simulations, we determined that the average energy of scattered photons in  $\Delta E$  was 181 MeV with a full width of 14 MeV.

We now examine the constraints on the elastic cross section imposed by the optical theorem and a dispersion relation. Using the optical theorem, we can write  $\text{Im}f(E, 0^\circ) = (k/4\pi)\sigma(E)$ , where  $\text{Im}f(E, 0^\circ)$  is the imaginary part of the elastic forward-scattering amplitude,  $k$  is the photon wave number, and  $\sigma(E)$  is the total photoabsorption cross section. There are no direct measurements of the total photoabsorption cross section in the  $\Delta$ -resonance region for  ${}^4\text{He}$ . However,  $\sigma(E)$  can be estimated on the basis of the value of  $\sigma_A/A$  obtained from measurements of  $\sigma_A$  on a large variety of targets.<sup>6</sup> For  ${}^4\text{He}$  this estimate gives  $\sigma = 0.45 \pm 0.07$  mb at 180 MeV, which is consistent with the value obtained directly from measurements of the photoemission of charged hadrons.<sup>7</sup> The lower bound on the cross section at  $0^\circ$  from the optical theorem is then  $[\text{Im}f(E, 0^\circ)]^2 = 0.11 \pm 0.03$   $\mu\text{b}/\text{sr}$ . With a knowledge of the total  ${}^4\text{He}$  cross section at all energies,<sup>6,8</sup> we have obtained the real part of  $f$  from a dispersion relation<sup>9</sup>:

$$\text{Re}[f(E, 0^\circ) - f(0, 0^\circ)] = \frac{E^2}{2\pi^2\hbar c} \text{P} \int_0^\infty \frac{\sigma(E')}{E'^2 - E^2} dE',$$

where  $f(0, 0^\circ) = -Z^2 e^2 M_A^{-1} c^{-2}$  is the Thomson limit and  $M_A$  is the nuclear mass. Because of the approximations involved at high energies and from use of indirect measurements of the total cross section in the  $\Delta$  region, a fairly large error was assigned to the calculat-

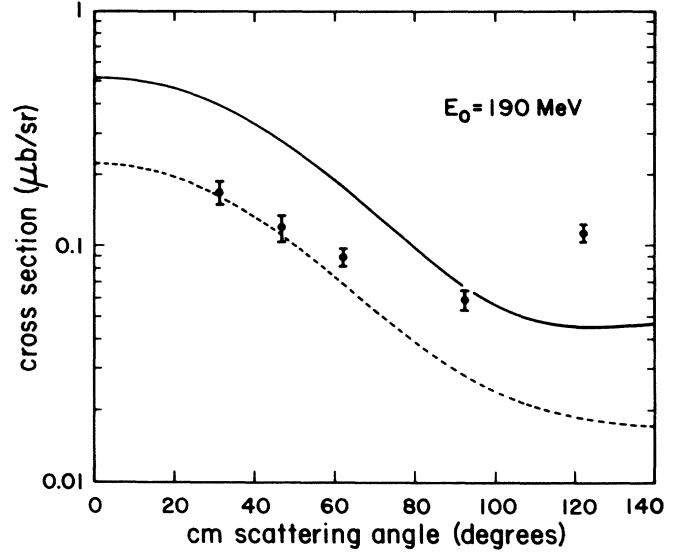


FIG. 4. The differential cross section at 180 MeV. Dots, measured data. Dashed line,  $[d\sigma(E, 0^\circ)/d\Omega] \times \frac{1}{2} \times (1 + \cos^2\theta) |F(q)|^2$ ;  $d\sigma(E, 0^\circ)/d\Omega$  is from dispersion relations. Solid line, calculation based on model of Ref. 1.

ed amplitude. The forward differential cross section obtained from the dispersion relations at an average energy of 180 MeV is  $|f(E, 0^\circ)|^2 = 0.27 \pm 0.10$   $\mu\text{b}/\text{sr}$ , which is consistent with the value of  $\sim 0.22$   $\mu\text{b}/\text{sr}$  obtained by extrapolation of our data from the  $30^\circ$  point to  $0^\circ$ . Both values are well above the lower limit established by the optical theorem. The extrapolation of the data was done by assuming the angular dependence to be that of an electric dipole,  $\frac{1}{2}(1 + \cos^2\theta)$ , times the square of the elastic-electron-scattering form factor, as was done in Ref. 3. As can be seen in Fig. 4, the agreement at forward angles is good but the prediction using this extrapolation is well below our data at backward angles. However, the validity of this approach for large angles is questionable since Compton-scattering cross sections at backward angles even for the proton are not reproduced by a single-multipole distribution.<sup>10</sup>

To study the energy dependence of the  $(\gamma, \gamma)$  cross section, we have modeled the pulse-height spectra at  $30^\circ$  on the basis of the previously described Monte Carlo technique, now assuming the energy dependence of the cross section to be the same as that at  $0^\circ$  deduced by use of the real and imaginary parts of  $f(E, 0^\circ)$ . The resulting shape produces better agreement with the data (Fig. 3) than the energy-independent model. There is no indication in the data of an energy dependence in the cross section at back angles. The data show no inelastic events above the  $\pi^0$ -decay-photon energies, which would appear as an abrupt increase in the observed spectra beginning 190

MeV below the end-point energy. We note that these data would only be sensitive to inelastic scattering to nuclear states with excitation energies less than 25 MeV. Contributions above this state would be masked by  $\pi^0$ -decay-photon background.

The only detailed calculations available at present for elastic photon scattering at intermediate energies were made in the context of the isobar-hole approach. The  $\Delta$ -hole model of Ref. 1 has been used to describe successfully pion-induced reactions and coherent  $\pi^0$  photoproduction and also to predict nuclear photoabsorption and Compton scattering at energies around the  $\Delta$  resonance. Discrepancies have been noted, however, in comparisons with the total photoabsorption cross section for light nuclei.<sup>1</sup> Figure 4 shows that the theoretical results for  ${}^4\text{He}(\gamma, \gamma){}^4\text{He}$  at 180 MeV are too high in the forward direction by about a factor of 2 and fail to reproduce the strong rise at back angles as indicated by the  $\theta_{\text{lab}} = 120^\circ$  data point. We note, however, that the calculation is not expected to be as reliable at 180 MeV as it would be nearer the peak of the  $\Delta$  resonance, which occurs at about 320 MeV for the free proton. In the model it was assumed that resonant contributions dominated, and therefore non-resonant contributions, which are less important at 320 than at 180 MeV, were treated less carefully.

For a wide range of angles and energies the fundamental  $(\gamma, \gamma)$  amplitudes on the proton are not known accurately, and are not fitted well by dispersion-relation fits.<sup>10</sup> Generally, forward-angle measurements are absent at all energies and data are particularly sparse near 180 MeV. Calculations for complex nuclei based on these elementary amplitudes will have corresponding errors.

As was pointed out in Ref. 1, the resonant nuclear photoabsorption cross section for  ${}^4\text{He}$  at energies somewhat below the resonance peak is dominated by coherent  $\pi^0$  photoproduction. No recent measurements are available at 180 MeV.

We have shown that a large NaI detector can be used to measure the nuclear-Compton-scattering cross section at forward angles. We conclude that the  $\Delta$ -

hole model which is optimized for higher energies does not describe the data well at 180 MeV. Better calculations and more data on complex nuclei and on the proton will be required to understand the nature of photon scattering in this energy region. We plan to extend our measurements to energies nearer the resonant peak in the order to test definitively the isobar-hole models.

It is a pleasure to acknowledge useful discussions with Dr. J. Ahrens, Dr. J. Koch, Professor E. Moniz, and Professor A. Nathan. We thank the staff at Bates Linear Accelerator for their invaluable assistance, and Professor A. Sachs and Nevis Laboratories for lending us their NaI detector. We would also like to acknowledge the participation of Dr. G. Ciangaru during the early stages of this experiment. This work was supported in part by National Science Foundation Grant No. PHY-8311277.

---

<sup>1</sup>J. H. Koch, E. J. Moniz, and N. Ohtsuka, *Ann. Phys. (N.Y.)* **154**, 99 (1984). We thank J. H. Koch for providing the predicted curve for 180 MeV.

<sup>2</sup>H. Genzel, M. Jung, R. Wedemeyer, and H. J. Weyer, *Z. Phys. A* **279**, 399 (1976).

<sup>3</sup>E. Hayward and B. Ziegler, *Nucl. Phys.* **A414**, 333 (1984).

<sup>4</sup>H. Arenhövel, M. Weyrauch, and P.-G. Reinhard, *Phys. Lett.* **155B**, 22 (1985).

<sup>5</sup>R. L. Ford and W. R. Nelson, EGS, Electron Gamma Shower Code, SLAC Report No. SLAC-210, 1978 (unpublished).

<sup>6</sup>C. Chollet, J. Arends, H. Beil, R. Bergere, P. Bourgeois, P. Carlos, J. L. Fallou, J. Fagot, P. Garganne, A. Lepetre, and A. Veysierre, *Phys. Lett.* **127B**, 331 (1983).

<sup>7</sup>H. Rost, University of Bonn Report No. IR-80-10, 1980 (unpublished).

<sup>8</sup>J. Ahrens, *Nucl. Phys.* **A446**, 229 (1985).

<sup>9</sup>M. Gell-Mann, M. L. Goldberger, and W. E. Thirring, *Phys. Rev.* **95**, 1612 (1954).

<sup>10</sup>I. Guiasu, C. Pomponiu, and E. E. Radescu, *Ann. Phys. (N.Y.)* **114**, 296 (1978).